NANO LETTERS

2008
Vol. 8, No. 6
1709-1712

Quantum Dot Microdrop Laser

J. Schäfer,[†] J. P. Mondia,[†] R. Sharma,[†] Z. H. Lu,[†] A. S. Susha,[‡] A. L. Rogach,[‡] and L. J. Wang*,[†]

Institute of Optics, Information and Photonics, Max-Planck Research Group, University of Erlangen-Nuremberg, 91058 Erlangen, Germany, and Photonics and Optoelectronics Group, Department of Physics and CeNS, Ludwig-Maximilians-University Munich, 80799 Munich, Germany

Received March 5, 2008; Revised Manuscript Received April 18, 2008

ABSTRACT

We report single-mode and multimode lasing from isolated spherical liquid microcavities containing CdSe/ZnS nanocrystal quantum dots. Lasing is observed at densities more than 2 orders of magnitude lower than previously demonstrated or theoretically predicted, assuming a uniform nanocrystal quantum dot distribution. Charged droplets, between 10 and 40 μm in size, are electrodynamically levitated and optically pumped. Substantial laser signals at low thresholds are measured from the directional emission normal to the pump beam, owing to the high Q cavity modes.

Semiconductor nanocrystal quantum dots (NQDs) have great potential for future photonic devices.[1] Strong three-dimensional charge carrier confinement makes them promising candidates for lasers in terms of lower pump powers, temperature stability, and spectral tunability. However, entering the strong confinement regime (i.e., core sizes <10 nm, where the spacing between the electronic states is larger than room temperature energy carriers) creates new loss mechanisms that hinder the buildup of lasing. One major loss factor is Auger recombination, which is intrinsically connected with the biexcitonic population inversion necessary for optical gain. Klimov et al. proposed to outplay Auger loss by using high NQD densities thus making the stimulated emission buildup time, τ_s, shorter than the biexcitonic Auger decay time, τ_2 ($\tau_s < \tau_2$). Thus they were able to propose a lower limit for the NQD volume fraction, ξ,[2]

$$\xi > \frac{4\pi n_r}{3\sigma_g c\beta} \tag{1}$$

where n_r is the index of refraction in the medium and c is the vacuum speed of light. The quantity ξ is defined as $4\pi n_0 R^3/3$, where n_0 and R are the NQD density and radius, respectively. The values of the gain cross section $\sigma_g \sim 2 \times 10^{-17}$ cm^2 for $R = 1.3$ nm and a coefficient $\beta \sim 5$ ps nm^{-3} were experimentally determined.[2] To date, NQD lasing for a variety of microcavities, including distributed feedback gratings,[3] silica microspheres,[4] and silica toroidal microcavities[5] as well as high-density NQD solution surrounding a fiber,[6] have been reported. All these systems satisfy the above minimum density condition.

Spherical microcavities are suitable candidates for microresonators because of their potentially high Q-factors and small mode volumes.[7] Microdrops in air form an almost perfect sphere with a smooth surface and have been used to demonstrate lasing from dyes, for example, in a microdrop liquid jet,[8] levitated in an electrodynamical (Paul) trap,[9] and on superhydrophobic surfaces.[10] The liquid sphere cavity allows large size tunability and doping flexibility and thus comprises a good test system for a laser gain medium such as NQDs. In this Letter, we report observation of room-temperature, low-threshold, single-mode and multimode lasing of low concentration CdSe/ZnS core−shell NQDs in a levitated micodrop optically pumped with a nanosecond system. Surprisingly, we achieved lasing for NQD volume fractions almost 2 orders of magnitude lower than the predicted minimum.

A schematic diagram of the experimental setup is shown in Figure 1. An electrodynamic endcap trap[11] is used to levitate the charged microdrops. An ac field applied to the two endcaps traps the charged droplet and four pairs of dc electrodes surrounding the endcaps are used for droplet positioning and gravity compensation. Typical endcap voltages and frequencies are 2 kV peak to peak and 300 Hz. The endcap trap is enclosed by a sealed grounded housing with four access ports. Droplets are injected through the top port via a home-built microdrop generator.[12] Additional charging by a simple fluid jet polarization technique results in droplet diameters of 10−50 μm with typical surface charges of 10^6 electrons. The trapped microdrop is optically pumped from the bottom port with 10 ns pulses from a frequency doubled Q-switched Nd:YAG laser at 532 nm and a repetition rate of 10 Hz. The laser beam diameter at the

* Corresponding author: lwan@optik.uni-erlangen.de.
[†] University of Erlangen-Nuremberg.
[‡] Ludwig-Maximilians-University Munich.

10.1021/nl080661a CCC: $40.75
Published on Web 05/10/2008

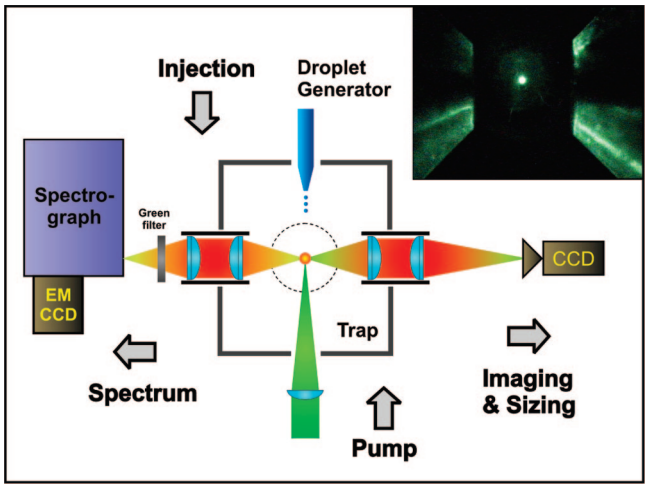

Figure 1. Schematic diagram of the experimental setup. An electrodynamic endcap trap is used to levitate a microdrop. The droplets are injected vertically from above the trap and the pump beam is incident vertically from below. The scattered light is collected on either side of the trap for imaging and spectral analysis. Inset: Picture of trapped microdrop.

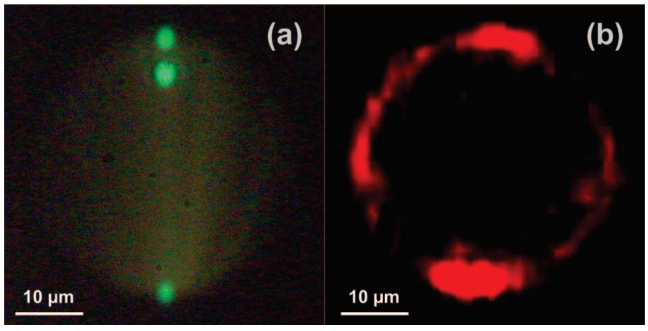

Figure 2. High-magnification images of a 40 μm droplet doped with NQDs, (a) under a green CW pump from the bottom and (b) under pulsed excitation, characteristic red lasing ring observed (with enhanced color contrast).

droplet is 1.3 mm ($1/e^2$). For initial alignment of the droplet in the trap, a lower power 532 nm continuous wave (CW) laser is employed. The side ports are used for spectral measurements, droplet imaging, and size determination.

The microdrop is composed of water-soluble CdSe/ZnS core−shell NQDs,[13] diluted in water and an additional 30% vol of glycerine in order to reduce evaporation. The CdSe core radius is 2.6 nm, yielding a photoluminescence (PL) emission peak at 625 nm with a specified quantum yield of 59%. The NQD concentration was varied between 1.3 and 2.6 μM.

A magnified image of a microdrop, pumped by a green CW laser is displayed in Figure 2a and shows the typical three glare spots of scattered light.[14] The droplet size is determined from interference fringes between the upper and lower glare spot.[15] At lasing condition well above threshold (pulsed excitation) a characteristic lasing ring around the circumference of the droplet can be observed. This is shown in Figure 2b, where the green excitation light is filtered out. At high enough pump powers NQDs from the entire surface contribute to the laser output. The droplet stability is strongly affected by the laser pulses requiring real-time tuning of the

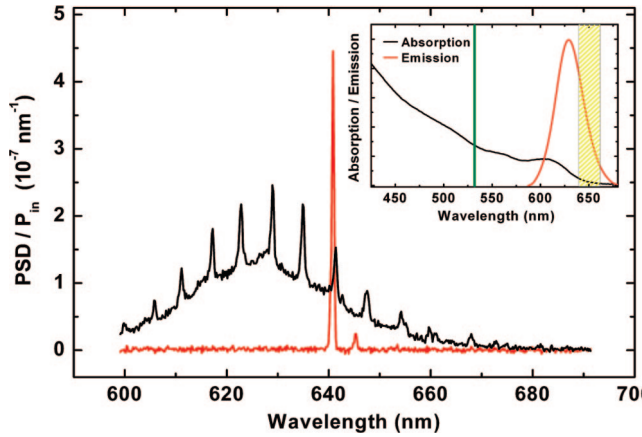

Figure 3. PL and lasing spectra of a 9 μm droplet with CdSe/ZnS NQDs: black curve (PL) exhibits WGM features; red curve represents single mode lasing. Power spectral density (PSD) is normalized to the cross-sectional pump power. Inset: absorption and emission spectra for CdSe/ZnS NQDs. Green line indicates pump wavelength, and yellow area marks gain region.

trap parameters to maintain a stable position to within a few micrometers.

Single-mode lasing was achieved for droplet sizes below 10 μm, where the spacing of the whispering gallery modes (WGMs) from the spherical cavity are comparable to the spectral gain region. This is shown for a typical 9 μm droplet in Figure 3. The PL spectrum (black curve) exhibits the characteristic WGM distribution as observed previously from silica and latex spheres coated with CdSe[16] and CdTe[17] NQDs, respectively. The inset of Figure 3 shows the absorption and emission spectra for our NQD solution. The green line represents the pumping wavelength and the yellow area highlights the region of optical gain, i.e., where population inversion can be attained. The red curve in Figure 3 represents the lasing behavior of the 9 μm droplet near threshold. The lasing action is almost entirely occupied by a single mode with an additional side mode emerging at higher powers. Another noticeable feature is a 0.5 nm blue shift of the main lasing mode with respect to the corresponding WGM, which is due to a slight evaporation of the microdrop induced by the pulsed pump beam.

The lasing threshold for the 9 μm droplet (2.6 μM) is at a pump fluence of 53 mJ/cm^2. Similar thresholds in solution have only been reported for CdSe/ZnS quantum rods;[6] the thresholds for dots were much higher ($\sim$ 1200 mJ/cm^2).[6] Stable lasing operation, before saturation, could be observed up to 100 mJ/cm^2. A careful calibration of our spectrometer enabled us to estimate the actual spectral distribution of the optical power radiated from the microdrop into our solid collection angle of 0.41 sr. In Figure 3 the power spectral density (PSD) collected from the droplet is normalized to the average input power (incident on the droplet cross section) in order to compare the PL and lasing signals. Note that lasing only happens within a thin surface layer containing $\sim$7% of the microdrop volume,[18] whereas all the NQDs in the droplet contribute to the PL signal.

For bigger droplets multimode lasing is observed. Figure 4 shows the standard threshold behavior for a 34 μm droplet

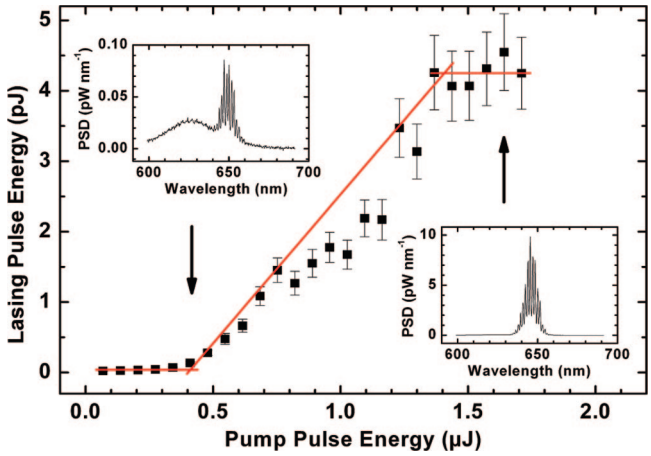

Figure 4. Lasing behavior of a 34 μm droplet with CdSe/ZnS NQDs. Each point represents the optical energy emitted from the droplet (over the lasing region of 630−660 nm) into the solid collection angle per pump pulse. The data are averaged from 20 exposures each covering 10 pulses. The error bars display the corresponding standard deviation. Insets: corresponding lasing spectra near the lasing onset (left) and near saturation (right).

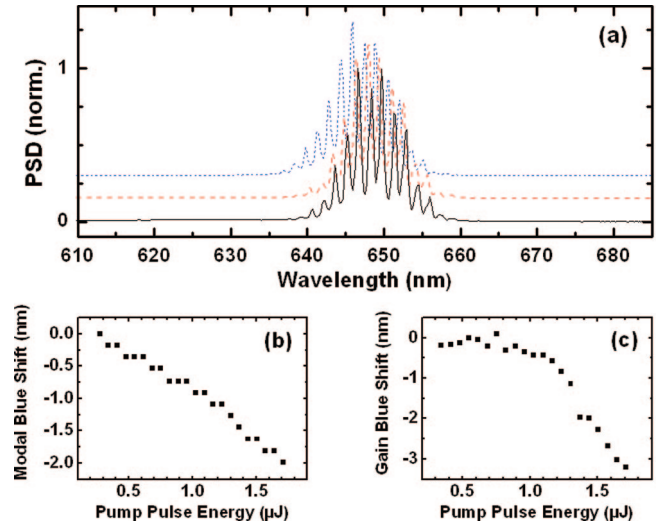

Figure 5. Blue shift behavior for increasing pulsed pump powers. (a) The black, red, and blue spectra (normalized to unity) correspond to pump pulse energies of 0.7, 1.0, and 1.4 μJ, respectively. (b) Blue shift of individual modes. (c) Blue shift of the gain region (center position determined by Gaussian fit of gain region).

(1.3 μM). It can be divided into three distinct regions. For pump energies below threshold ($\sim$ 0.4 μJ, relates to fluence of 44 mJ/cm^2) the broad PL emission spectrum typical for these NQDs is observed. At threshold, initial laser peaks emerge from the characteristic gain region (left inset). Changing the concentration from 1.3 to 2.6 μM for droplets of equal size did not change the threshold level. However, there seems to be a slight reduction of the threshold fluence with increasing droplet size. Above threshold, the lasing signal increases linearly with pump pulse energy. As a guide to the eye, a line is drawn in the diagram to show this linear rise. A group of data points in the central region does not follow the line. This is due to the fact that good coupling depends critically on the exact droplet position. Finally, saturation sets in for pump pulse energies above 1.35 μJ, where a typical spectrum is shown in the right inset. The larger error bars underline the decreasing droplet stability at higher excitation power, which cannot be completely suppressed by the stabilizing procedure previously mentioned.

At larger pump powers, we also observe a blue shift of the lasing modes and the gain profile. Figure 5a shows three spectra for pump pulse energies in the linear lasing region (0.7−1.4 μJ). The blue shift of the individual modes is plotted in Figure 5b and can again be accounted for by slight droplet evaporation. In addition, there is a nonreversible blue shift of the gain profile starting near lasing saturation. This is represented in Figure 5c, which shows the center position of a Gauss envelope fitted to the group of lasing modes for each pump energy. This effect is caused by radiation-induced NQD photo-oxidation.[19] Note that similar modal shifts are observed for long exposure times at fixed pump powers well within the lasing region; however the shift of the gain profile did not change.

We observed dramatic blue shifts of the gain profile from water-soluble core-only CdTe NQDs[20] of similar transmission wavelengths ($\sim$630 nm). For these NQDs, shifts of the gain profile are greater than 10 nm and a large signal drop sets in at pump pulse energies of $\sim$0.4 μJ. In comparison, the core−shell NQDs show strong pump pulse resistances up to 1.5 μJ. Despite clear WGM fluorescent features, the core-only NQDs did not lase. We believe that this can mainly be attributed to the high susceptibility to photo-oxidation.[19] Moreover, the lower PL quantum yield of the core-only structure[21] necessitates higher pump powers to reach lasing threshold. Hence we conclude that the core−shell structure significantly improves the NQD lasing potential.

Our large signals and comparatively low lasing thresholds are likely a result of the microdrop cavity geometry. Unlike solid microspheres coated with NQDs[4] or even NQD solution surrounding a fiber,[6] lasing from the microdrop excites not only surface NQDs but also higher order modes which have penetrated into the surface.[22] Although higher order modes have a lower Q-factor, they often have larger lasing signals, because more gain material is excited. Due to their intrinsically high sphericity and surface smoothness, liquid microspheres can have potentially high Q-factors ($\sim 10^6$).[23] The Q-factor of the microdrops used in the experiment is lowered owing to field-induced shape distortions from the pump pulses.[24] From spectral measurements, which are limited by the resolution of our spectrometer, we determined a lower limit, $Q = 6.5 \times 10^3$.

It is particularly interesting to note that the observation of lasing occurs at a NQD volume fraction of $\xi = 0.006\%$, significantly lower than the previously observed or predicted threshold at $\xi \sim 0.2\%$. The origin of this discrepancy is unclear and is under further investigation. However, from eq 1, we see that only two parameters can account for this inconsistency, the measured value of ξ or the gain cross section σ_g. Certainly one possibility is that our assumption of a uniform NQD distribution in the droplet is not valid and there is a strong accumulation near the charged surface, where lasing happens. Another possibility is that our NQDs, which have twice the core size (R = 2.6 nm) than in the

cited paper,[2] exhibit a higher gain cross section and thus a lower threshold concentration. However, in order to reach comparable values of ξ, we calculated that σ_g must increase by at least 23 times. Consequently, the widely used concentration threshold condition (eq 1) may not apply for the experimental case reported here.

We have demonstrated a flexible all-liquid, electrodynamically levitated spherical microlaser based on low concentrations of CdSe/ZnS NQDs. Different cavity sizes have been studied achieving single mode lasing for diameters $<10\ \mu$m and more stable multimode operation for bigger droplet sizes up to 41 μm. Measurements with CdTe core-only NQDs underline the important role of the shell for accomplishing lasing by protecting the core from photo-oxidation. We believe even lower thresholds can be achieved with type-II NQDs, where Auger recombination can be eliminated by accessing single-exciton gain.[25] Owing to its simple, solution-based sample preparation and high-Q resonating property, our system is a versatile candidate for future investigations of the lasing properties of such novel gain media.

Acknowledgment. LMU contributors acknowledge financial support of the DFG via the "Nanosystems Initiative Munich (NIM)".

References

(1) Alivisatos, A. P. *Science* **1996**, *271*, 933.
(2) Klimov, V. I.; Mikhailovsky, A. A.; Xu, S.; Malko, A.; Hollingsworth, J. A.; Leatherdale, C. A.; Eisler, H.-J.; Bawendi, M. G. *Science* **2000**, *290*, 314.
(3) Eisler, H.-J.; Sundar, V. C.; Bawendi, M. G.; Walsh, M.; Smith, H. I.; Klimov, V. *Appl. Phys. Lett.* **2002**, *80*, 4614.
(4) Snee, P. T.; Chan, Y.; Nocera, D. G.; Bawendi, M. G. *Adv. Mater.* **2005**, *17*, 1131.
(5) Min, B.; Kim, S.; Okamoto, K.; Yang, L.; Scherer, A.; Atwater, H.; Vahala, K. *Appl. Phys. Lett.* **2006**, *89*, 191124.
(6) Kazes, M.; Lewis, D. Y.; Ebenstein, Y.; Mokari, T.; Banin, U. *Adv. Mater.* **2002**, *14*, 317.
(7) Vahala, K. J. *Nature* **2003**, *424*, 839.
(8) Qian, S.-X.; Snow, J. B.; Tzeng, H.-M.; Chang, R. K. *Science* **1986**, *231*, 486.
(9) Tona, M.; Kimura, M. *J. Phys. Soc. Jpn.* **2000**, *69*, 3533.
(10) Kiraz, A.; Sennaroglu, A.; Doğanay, S.; Dündar, M. A.; Kurt, A.; Kalaycıoğlu, H.; Demirel, A. L. *Opt. Commun.* **2007**, *276*, 145.
(11) Schlemmer, S.; Illemann, J.; Wellert, S.; Gerlich, D. *J. Appl. Phys.* **2001**, *90*, 5410.
(12) Schäfer, J.; Mondia, J. P.; Sharma, R.; Lu, Z. H.; Wang, L. J. *Rev. Sci. Instrum.* **2007**, *78*, 066102.
(13) Evident Technologies, 216 River Street, Suite 200, Troy, New York 12180, www.evidenttech.com.
(14) Tona, M.; Kimura, M. *J. Phys. Soc. Jpn.* **2002**, *71*, 425.
(15) Damaschke, N.; Nobach, H.; Nonn, T. I.; Semidetnov, N.; Tropea, C. *Exp. Fluids* **2005**, *39*, 336.
(16) Artemyev, M. V.; Woggon, U.; Wannemacher, R.; Jaschinski, H.; Langbin, W. *Nano Lett.* **2001**, *1*, 309.
(17) Rakovich, Y.; Yang, L.; McCabe, E. M.; Donegan, J. F.; Perova, T.; Moore, A.; Gaponik, N.; Rogach, A. L. *Semicond. Sci. Technol.* **2003**, *18*, 914.
(18) Barnes, M. D.; Whitten, W. B.; Arnold, S.; Ramsey, J. M. *J. Chem. Phys.* **1992**, *97*, 7842.
(19) Nazzal, A. Y.; Wang, X.; Qu, L.; Yu, W.; Wang, Y.; Peng, X.; Xiao, M. *J. Phys. Chem. B* **2004**, *108*, 5507.
(20) Gaponik, N.; Talapin, D. V.; Rogach, A. L.; Hoppe, K.; Shevchenko, E. V.; Kornowski, A.; Eychmüller, A.; Weller, H. *J. Phys. Chem. B* **2002**, *106*, 7177.
(21) Hines, M. A.; Guyot-Sionnest, P. *J. Phys. Chem.* **1996**, *100*, 468.
(22) Eversole, J. D.; Lin, H.-B.; Campillo, A. J. *J. Opt. Soc. Am. B* **1995**, *12*, 287.
(23) Arnold, S.; Folan, L. M. *Opt. Lett.* **1989**, *14*, 387.
(24) Tzeng, H. M.; Long, M. B.; Chang, R. K.; Barber, P. W. *Opt. Lett.* **1985**, *10*, 209.
(25) Klimov, V. I.; Ivanov, S. A.; Nanda, J.; Achermann, M.; Bezel, I.; McGuire, J. A.; Piryatinski, A. *Nature* **2007**, *447*, 441.

NL080661A